Assessment of propeller induced properties and active flow control using multiple image-based measurement systems

Eric W.M. Roosenboom[1], Reinhard Geisler[1], Janos Agocs[1], Daniel Schanz[1], Thorsten Weikert[1], Tania Kirmse[1] and Andreas Schröder[1]

[1] DLR (German Aerospace Center), Institute of Aerodynamics and Flow Technology, Department Experimental Methods, Goettingen, Germany
Eric.Roosenboom@dlr.de

ABSTRACT

Multiple optical measurement techniques have been applied for the investigation of a propeller-wing wind tunnel model. The (half) wind tunnel model is equipped with a nine bladed propeller and its wing has active Coanda blowing over the whole span of the wing. The aim of the investigation is to gain understanding of the flow phenomena, especially the interaction of the periodic propeller slipstream with the Coanda blowing. The optical measurement techniques used are: stereoscopic Particle Image Velocimetry (for investigating the flow field behind the propeller till the end of the wing), mono Particle Image Velocimetry (for the investigation of the Coanda blowing), Background Oriented Schlieren (for investigating the density gradients in the propeller slipstream) and Projected Pattern Correlation (for the blade torsion and deformation). This paper discusses the application of these methods during a single wind tunnel entry in an industrial wind tunnel facility.

INTRODUCTION

Non-intrusive image-based measurement techniques are advantageous for the investigation of propeller flows [1] and are particularly useful for the investigation of effects such as thrust reverse [2] or propeller slipstream structures [3-4]. For propeller blade investigations techniques as Pressure Sensitive Paint [5] (for blade forces and moments) and oil film interferometry (for transition detection and skin-friction measurements) [6] are under development and have been shown to be feasible in industrial applications. Datasets obtained from advanced measurement techniques are of eminent importance for the validation of numerical codes [7]. In particular, the simultaneous measurement of velocity and propeller bending should be pursued in order to determine any influence of the modified blade orientation on the velocity field [8] The German research project 'Bürgernahes Flugzeug (BNF)' (translated: community friendly aircraft) is dedicated to the design of a quiet, efficient, short take-off and landings (QESTOL) aircraft which should alleviate cities and their residents from aircraft noise [10-14]. In order to enable short take-off and landings the aircraft is equipped with a propeller, in addition high lift capabilities are provided by active flow control using Coanda blowing. A 3D drawing of the model is given in Fig. 1. A close-up of the Coanda blowing is shown in Fig. 2. The various experimental aerodynamic aspects of the propeller behavior (slipstream effects, active blowing, bending and torsion etc.) are investigated within the DLR project 'SAMURAI', dedicated to the simultaneous application of multiple image-based measurement techniques, such as (stereoscopic and tomographic) Particle Image Velocimetry (PIV), Background Oriented Schlieren (BOS), Projected Pattern Correlation (PROPAC), Temperature and Pressure Sensitive Paint

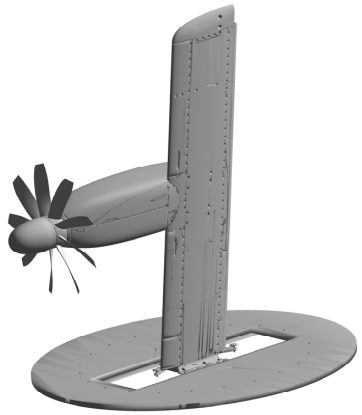

Figure 1 3D view of the BNF wind tunnel model.

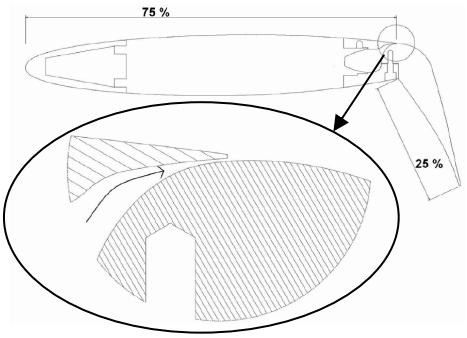

Figure 2 Close-up of the Coanda blowing region on the wing (Ref. 9).

(TSP/PSP) and Acoustic Array techniques. These image-based measurement techniques have been applied for the investigation of the propeller effects of the BNF aircraft, and the investigation of the active Coanda blowing. The resulting datasets will be used for a future validation of CFD results. The measurements are intended to provide simultaneous data on various propeller aspects, such as the flow and density gradient distributions in the propeller slipstream, the bending and torsion of the propeller blades at specified settings. Each of these properties is of importance for a solid validation. The present paper discusses several measurement techniques which have been applied during one wind tunnel entry for the investigation of several propeller induced properties. The propeller slipstream and the active flow control have been analyzed with stereoscopic and mono Particle Image Velocimetry (PIV), respectively. The helical structures at the inboard section of the propeller slipstream have been visualized with the Background Oriented Schlieren (BOS) method. Finally, the propeller blade bending and torsion are investigated using Projected Pattern Correlation (PROPAC).

MEASUREMENT SET-UP

A. Wind tunnel and wind tunnel model

The measurements are performed in the DNW-NWB low speed wind tunnel facility in Braunschweig (Germany). The closed test section has a cross-sectional area of 3.25 x 2.8 m^2. The wind tunnel is used in a closed test section configuration and a contraction ratio of 1:5.6. The BNF wind tunnel model is a half model (wing span about 1.7 m) equipped with a propeller (diameter 0.66 m) and active flow control by means of Coanda blowing over the gapless flap. The Coanda blowing consists of 3 blowing channels within the model, each of which can be individually controlled. The cruise angle of attack is -5 deg. The propeller blade pitch angle is 28 deg (at 75% of propeller radius). For the wind tunnel measurements the wind tunnel velocity and the propeller revolutions will remain fixed. The measurement parameters are listed in Table 1. The Coanda blowing within the wind tunnel model is performed using pressurized air in three sections along the span. Initially, uniform blowing with a pressure in the plenum of 0.55 bar in each section was anticipated. It turned out during the measurement campaign that the pressure was not sufficient to ensure attached flow over the flap. With some time-consuming trial and error, the mid-section blowing had to be increased to 1.8 bar at which attached flow occurred. Later investigations of the internal blowing channel revealed that a small ragged edge was responsible for the irregular blowing at the mid span section. The whole set-up and execution of the measurement campaign was performed in less than 10 wind tunnel days.

Table 1 Measurement settings

Parameter	*Value*
Angle of attack	-5 deg
Wind tunnel velocity	51 m/s
Propeller blade pitch angle ($\beta_{0.75}$)	28 deg
Propeller diameter	660 mm
RPM	7144
Advance ratio	0.649

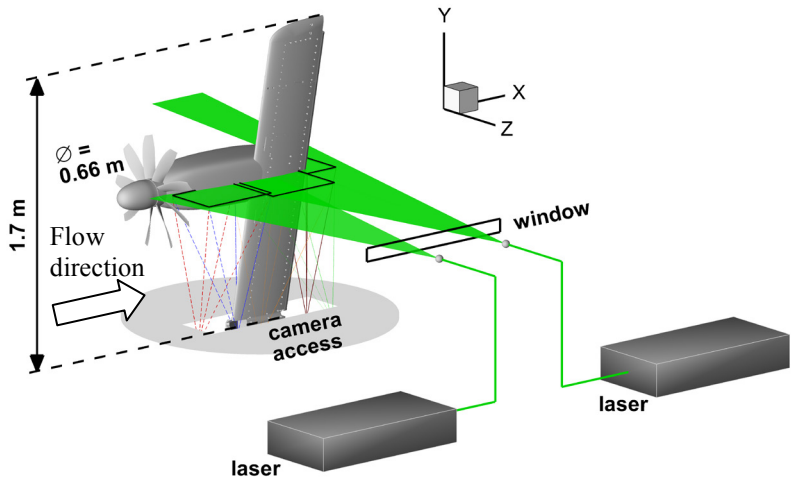

Figure 3 PIV Set-up in wind tunnel (dimensions in proportion).

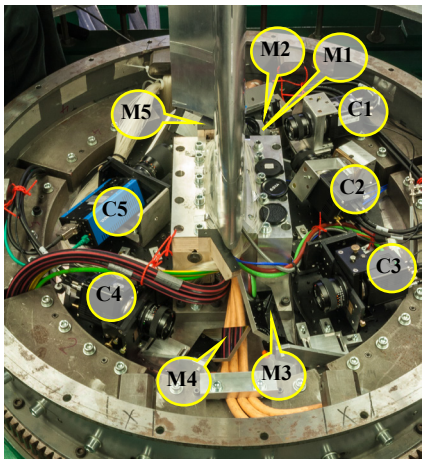

Figure 4 PIV camera arrangement.

B. Particle Image Velocimetry (PIV)

The propeller slipstream has been investigated with a double stereoscopic Particle Image Velocimetry (PIV) set-up. An overview of the PIV set-up is presented in Fig. 3. Homogeneous distribution of seeding (DEHS particles with an average diameter of 1 µm) was ensured by inserted seeding particles downstream of the model. A dedicated hose of the seeding system was directed through the Coanda blowing system in order to allow sufficient seeding in the blowing region. Unfortunately since the recent renovation of the DNW-NWB facility only limited amounts of seeding are

allowed. The combined field of view of both PIV systems visualizes the slipstream from just behind the propeller (Cameras C2 and C4) to end of the engine pod (Cameras C1 and C3), see Fig. 4. The main reason for arranging the cameras in the cramped space at the wing root is that it offers the ability to rotate the cameras simultaneously with the angle of attack of the wind tunnel model without requiring an additional calibration. The active blowing has been measured with a mono-PIV set-up (Camera 5). All cameras are annotated C1-5 in Fig. 4; corresponding mirrors are annotated M1-5. The lenses (all Carl Zeiss) used were: 50 mm for Camera 2, 35 mm for Cams 1, 3 and 4 and 135 mm for Camera 5. Four PCO Edge sCMOS cameras (2560 x 2160 pixel) have been used for both stereoscopic measurements, a PCO 4000 CCD camera (4008 x 2672 pixel) for the mono-PIV measurements of the flap blowing. For the laser light sheet generation two double pulse Nd:YAG laser systems (BigSky CFR and Spitlight 1000) were used simultaneously for the illumination of the extended field of view. The laser and camera systems were triggered with a TTL signal from the propeller (one signal per revolution).

C. Background Oriented Schlieren (BOS)

The BOS method has been applied for determining instantaneous distributions of the density gradients in the propeller slipstream. A random background dot pattern was illuminated by diffuse scattered pulsed Nd:YAG laser in order to reduce laser speckle noise. The illumination can be seen in Fig. 5. The dot pattern has been recorded with an additional PCO 4000 CCD camera (4008 x 2672 pixel). The BOS imaging consisted of recording wind off images, followed by a recording of the dot pattern in double-frame mode, with an appropriate (i.e. adapted to the convection velocity of the propeller tip vortices) pulse delay. This allows to either correlate the results obtained at the two time instances (resulting in density gradient variations), or to correlate each of the illuminations with the reference image. Results of both approaches will be discussed.

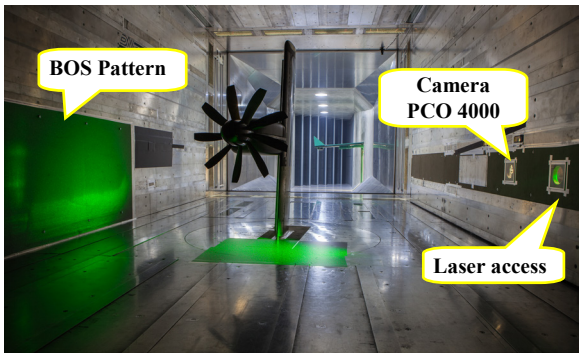

Figure 5 Illumination of BOS pattern.

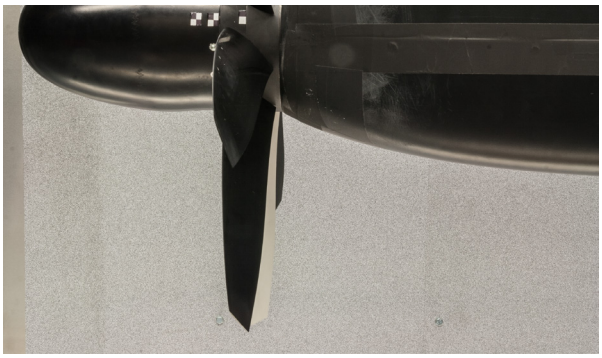

Figure 6 BOS pattern.

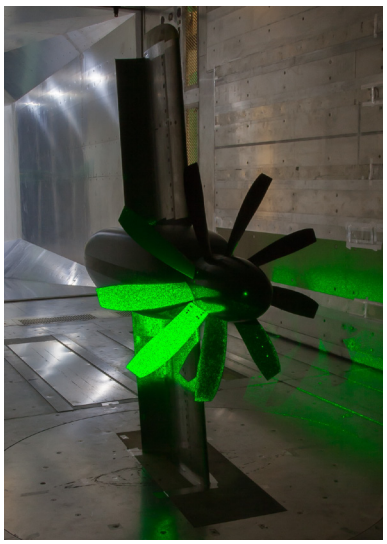

Figure 7 Propeller with projected pattern.

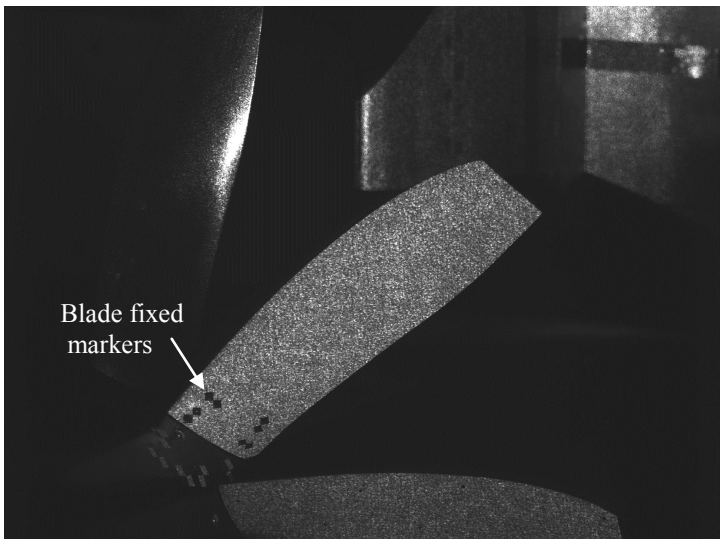

Figure 8 Sample camera image of the blade with reference markers and projected pattern.

D. Projected Pattern Correlation (PROPAC)

Information on the actual bending and torsion of the propeller blades are required for an accurate CFD analysis as any deviation from a rigid stiff propeller blade may induce slightly different associated pressure and velocity field distributions. In the current paper the 3D-surface of the blade is determined with the Projected Pattern Correlation

(PROPAC) technique (Fig. 7). The dot pattern was generated with a gobo projector and imaged with a stereo camera system of AVT GX-3300 CCD cameras (3296 x 2472 pixel). The resolution of the camera was binned to 2MP in order to achieve an acquisition frame rate of 20 Hz. The pulsed laser used as light source of the projector ensures a sufficient illumination within short light pulses to avoid blade movement effects. The measured blade was painted white which further improves the illumination efficiency. Because of the projective application of the random pattern on the wing the pattern is fixed in space and the blades moves through the pattern. Additional markers were applied in the root area of the blade as blade fixed reference, see Fig. 8.

RESULTS

The objectives of the measurements are multifold: the measurement techniques are used to supplement each other in order to provide experimental data on important propeller aspects. In addition, the specific design of the QESTOL aircraft with active blowing also requires an investigation. As mentioned before the regular active blowing parameter in the mid span section had to be adjusted to 1.8 bar, as opposed to 0.55 bar in the root and tip section. This setting enabled attached flow over the flap in the propeller slipstream. Significant, unscheduled, wind tunnel time was spent on determining appropriate settings for the blowing parameters. Essentially the remaining test matrix was a compromise between obtaining the required measurement data while maintaining qualitative useful aerodynamic data. In addition, the wind tunnel campaign serves as one of the first campaigns with simultaneous application of advanced measurement techniques. The foremost priority is the harmonization between the various measurement techniques. The main parameters during the measurements are listed in Table 1. The results of (some of) the applied various measurement techniques are discussed in this section.

A. Particle Image Velocimetry

Both stereoscopic and mono Particle Image Velocimetry has been applied. The results of the propeller slipstream measurement will be used for a CFD validation and therefore all velocity components are of interest. The active flap blowing will be primarily investigated for attached or detached flow and mono PIV is sufficient to determine the state of the flow. All data has been analyzed with PIVview using multigrid interrogation with image deformation (Final window size 32 pixel with 50% overlap). The combined field of view of the stereoscopic set-up is approximately 835 by 320 mm (with a vector resolution of 2.66 mm); the field of view for the mono camera is 217 by 270 mm (with a vector resolution of 0.56 mm). Figure 9a presents the averaged flow field distribution over 1000 instantaneous datasets allowing a statistically relevant result. The propeller slipstream is captured and the axial velocity is the highest at the trailing edge of the wing. Since the result was obtained as one of the first measurements (e.g. without the internal channel blowing adjustments), the flow at the flap is separated, with a small vortex at the flap tip location. The corresponding RMS values are shown in Fig. 9b. Here the individual tip vortices and wake traces can be clearly seen in the propeller slipstream, as well as the separated region over the flap, apart from a very small region close to the flap generated by the Coanda blowing. Due to the specific propeller (blade) design, the slipstream has higher convection velocities as the tip vortices. At the position of the wing leading edge the inner part of the propeller slipstream has convected further as the tip vortices. The tip vortices now become entrained between the free stream flow and the highly accelerated slipstream. The tip vortices are forced to roll-up in pairs.

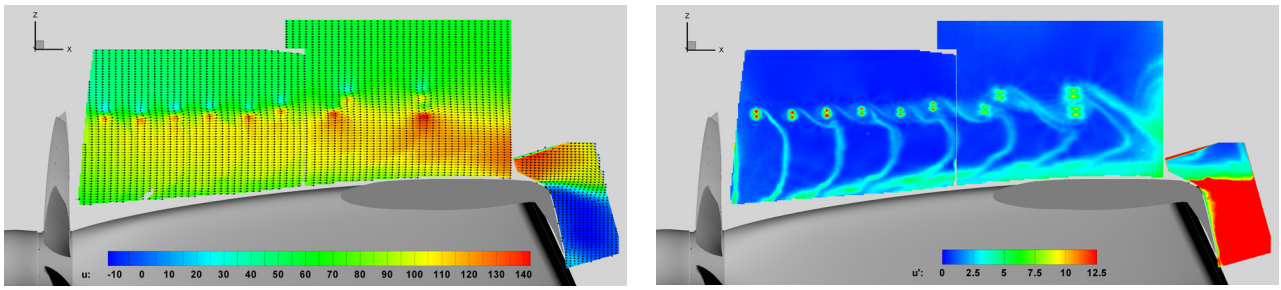

(a) Average velocity distribution (b) RMS velocity distribution

Figure 9 Results obtained with averaging over 1000 instantaneous data sets (Blowing 0.55 bar in all channels). Only 10% of the vectors are shown.

From the initial PIV measurements, as well as from surface pressure measurements, it was immediately clear that the active Coanda blowing was not behaving appropriately. Various unscheduled extra tests were performed to tune and optimize the blowing parameters. However, due to these additional tests the remaining wind tunnel program had to be reduced. Therefore, it was decided to reduce the number of snapshots for the PIV measurements: the remaining results are averaged over 50 samples and consequently no RMS data will be presented.

The evolution of the vortex and the rolling of the vortex are investigated in more detail in the results of the phase-locked

PIV measurements in Fig. 10. One blade-to-blade passage (40 deg) has been measured at 5 deg intervals, where 10 deg intervals are shown, each with 50 snapshots. One of the interesting observations that can be made is that the tip vortex locations are distinct, but that the upper part of the associated blade wake traces (with a mild negative vorticity) tends to move towards the next vortex. The previously identified vortex roll-up can be clearly detected at the leading edge region. The interaction of the various shearlayers and the onset of the vortex roll-up is visible in the consecutive results. The roll-up of two subsequent vortices is then maintained further downstream. The nacelle induced vortex seems to have only a mild influence on the wing boundary layer and it may therefore be assumed that there will be only a small periodic effect on the active blowing in the flap region

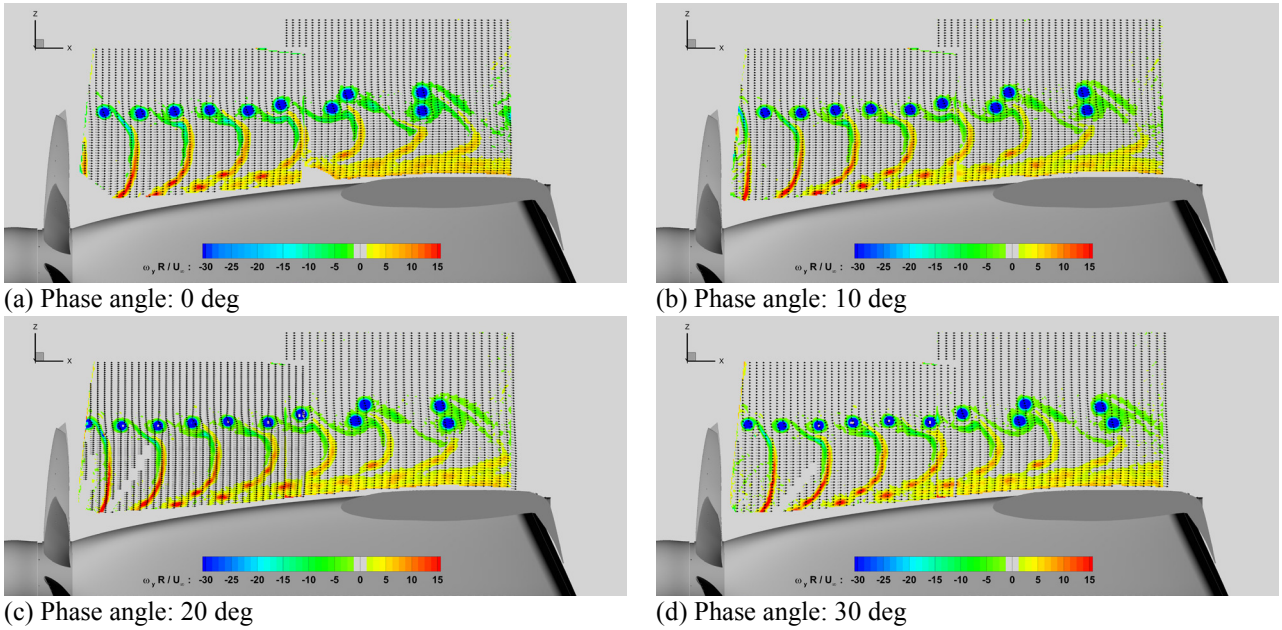

(a) Phase angle: 0 deg (b) Phase angle: 10 deg

(c) Phase angle: 20 deg (d) Phase angle: 30 deg

Figure 10 PIV (normalized) vorticity results of 1 blade-to-blade rotation with at 10 deg phase difference (intermediate results at 5 deg not shown.) Only 10% of the vectors are shown.

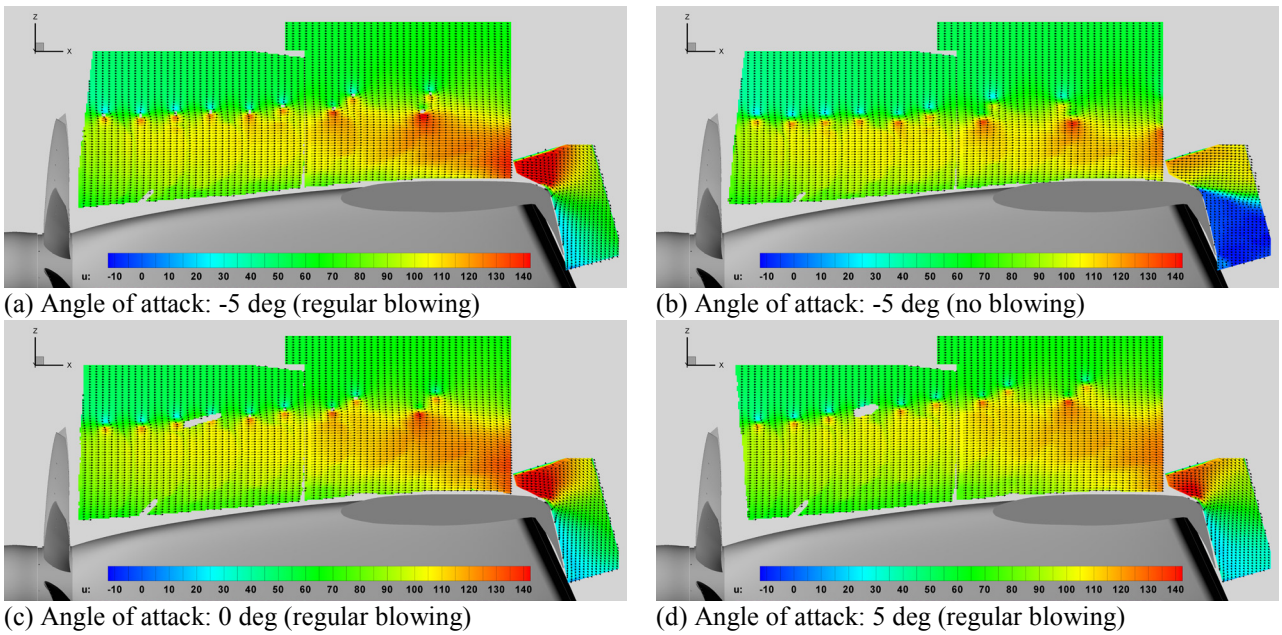

(a) Angle of attack: -5 deg (regular blowing) (b) Angle of attack: -5 deg (no blowing)

(c) Angle of attack: 0 deg (regular blowing) (d) Angle of attack: 5 deg (regular blowing)

Figure 11 PIV results (axial velocity) at several angles of attack, and compared to "blowing off" (at angle of attack of -5 deg) Only 10% of the vectors are shown.

The cruise angle of attack of the wing design of the QESTOL aircraft is at -5 deg. The influence of an angle of attack increase is presented in Fig. 11. The effect on the propeller slipstream is minimal, in fact only at the transition from the wing to the flap the suction peak is seen to decrease and shift forward. The effect on the active blowing (attached flow) is accordingly more relevant for the lower angles of attack. A comparison with no blowing (Fig. 11b) indicates that the

flow is separated and that the suction region (at the wing trailing edge flap leading edge) is significantly decreased. It also shows that the slipstream velocity is larger for active blowing and a larger part of the propeller slipstream is convecting over the suction side of the wing due to increased lift coefficients (up to $\alpha = 0$ deg). The increase in the angle of attack also indicates that the nacelle causes the slipstream to increase in thickness. In addition, the nacelle induced separation causes the flow over the wing to reattach further downstream.

B. Background Oriented Schlieren

The regular BOS evaluation (i.e. correlation of images of a flow containing a density gradient with a reference image) is sensitive to temperature gradients (as these may cause additional density gradient) as well as to vibrations (these may cause an extra artificial displacement). This implies that at performing BOS measurements in wind tunnels both sources of error need to be excluded, if quantitative density (gradient) results are required. If however only a quantitative visualization is pursued, then it might be sufficient to correlate two images at a given time delay (similar to double-pulsed PIV images). Figure 12 shows two BOS results obtained at two different phase angle positions during one wind tunnel run. Each of the results is an average over 20 instantaneous BOS gradients at phase locked blade positions and is obtained by correlating the BOS image with a reference image of the BOS pattern. Due to small expansion or contraction in the continuously running wind tunnel an additional shift is introduced in the BOS results obtained at later time instants. Figure 12a and 12b show the result with a pixel shift of 0.28 and 0.47 pixel subtracted, respectively (obtained from a region without density gradients). For full appreciation of the helical and slipstream data, combined PIV and BOS results are shown in Fig. A; and Animation 1 in Appendix A shows simultaneous PIV and BOS results.

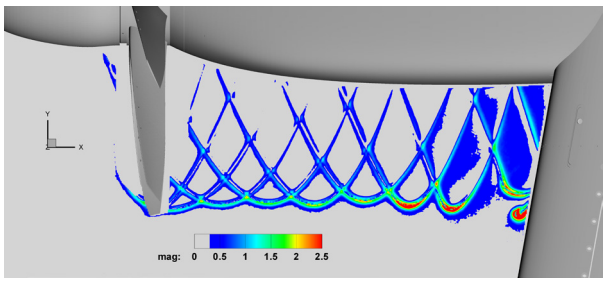

(a) Phase angle: 0 deg (with 0.28 pixel shift subtracted)

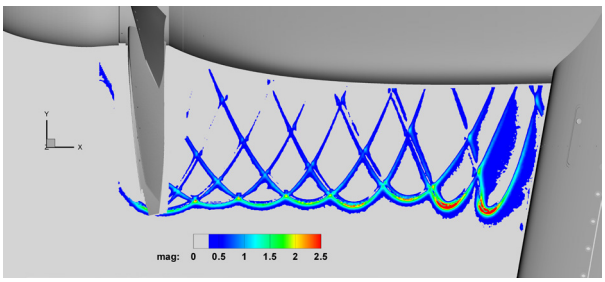

(b) Phase angle: 35 deg (with 0.47 pixel shift subtracted)

Figure 12 Regular BOS results (correlation with reference image).

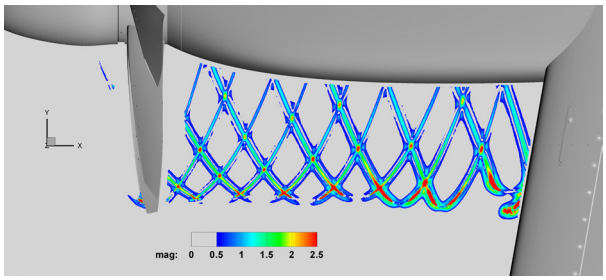

(a) Phase angle: 0 deg

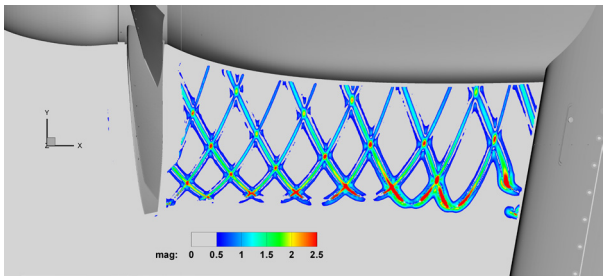

(b) Phase angle: 10 deg

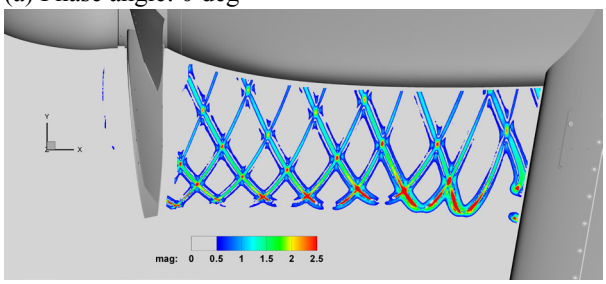

(c) Phase angle: 20 deg

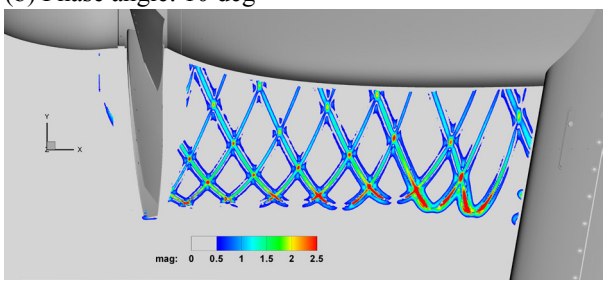

(d) Phase angle: 30 deg

Figure 13 BOS results of 1 blade-to-blade rotation with a 10 deg phase difference.

The apparent shift can be suppressed by correlating the double images obtained at an appropriate time delay (corresponding to approximately the vortex convection velocity). This results in density gradient variations, but still allows a qualitative visualization of the propeller slipstream [4]. BOS results at several phase angle positions are given in Fig. 13. The projected area of the BOS results is located in the propeller symmetry plane and in the plane of the wing

(see also Fig. 5 and Fig. A). The results are all obtained by correlating double-frames and averaging over 20 samples at one phase locked propeller blade position. Since BOS integrates by definition over the light path, the 3D helical slipstream is projected and upward and downward moving structures are superimposed. Projected helical paths orientated \\ are located above the wing; and paths orientated // are located below the wing. The magnitude of the density gradient variations is displayed and a threshold value of 0.5 is selected so that the slipstream stands out from the background. The propeller blade tip vortices behave like a helix for about one radius behind the propeller. Part of the structures at the valley of the parabola seem missing or below the threshold value, actually in these regions the density gradient variations are shallow and therefore are not visible (note that these missing parts are visible in Fig. 12). It can also be seen that the helical slipstream becomes stronger after one radius behind the propeller. The BOS results are projection of the helical vortical structures in the propeller slipstream in the symmetry of the propeller. The presence of the wing will induce a low pressure region at its leading edge which causes a disjunction of the helical tip vortex. This disjunction is clearly visible in the slipstream structures just in front of the wing leading edge in Fig. 13.

C. Projected Pattern Correlation

A stereoscopic camera set up allows the use of the evaluation principles and algorithms of the Image Pattern Correlation Technique (IPCT), also known as Digital Image Correlation (DIC) [15]. It combines image correlation algorithm also used for PIV and BOS evaluation to find corresponding areas in the different camera views. A triangulation of the point correspondences based on the stereo camera calibration delivers the 3D-coordinates of the measured surface in the next step. Due to the projective application of the random pattern, the pattern is shifted with respect to the measured surface as well. Nevertheless a reconstruction of the 3D-surface for the single stereo pairs is possible. As distinguished from IPCT/ DIC, where the pattern is fixed to the surface, a direct deformation measurement by a direct correlation of different time steps or deformation conditions is not possible. The deformation is determined by the subtraction of a reference surface from the deformed surface. Hence the deformation is calculated only in a defined direction and deformations in the perpendicular plane will be neglected.

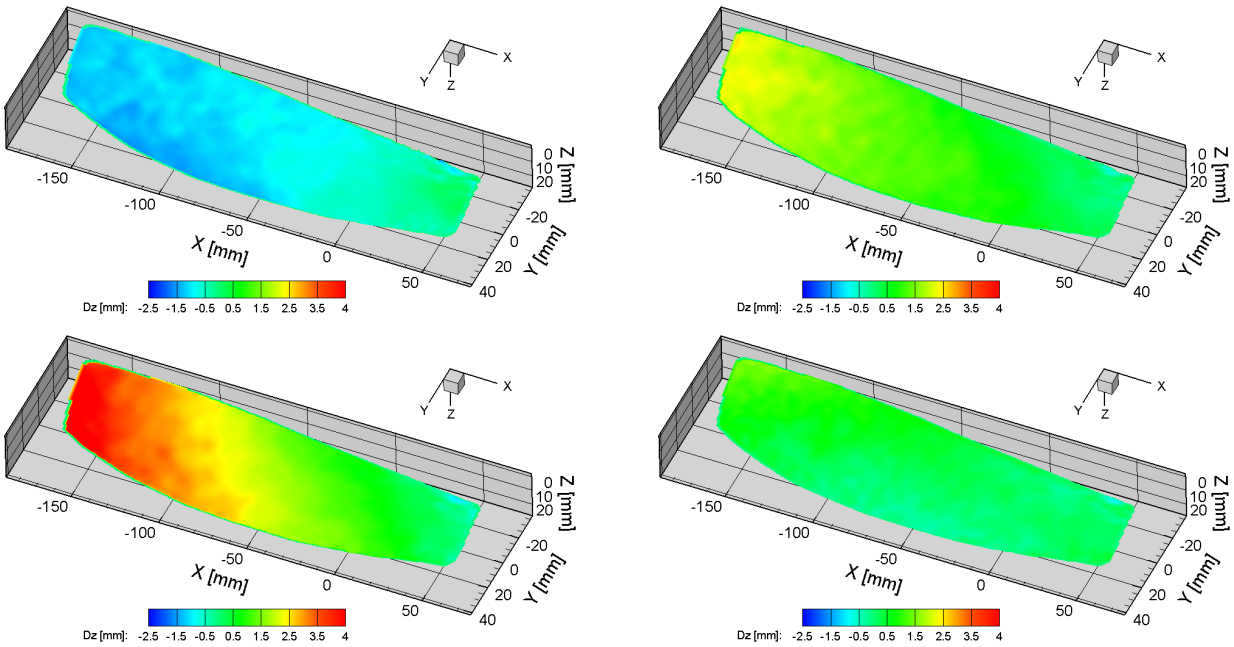

Figure 14 PROPAC results of 4 consecutive recordings at α = -5 deg and 5105 RPM.

Figure 14 shows sample results of 4 consecutive stereo recordings with a propeller speed of 5105 RPM and α = -5 deg. Because of the noisy rising edge of the incoming trigger of the propeller TTL signal, a triggered phase locked recording was not possible for the current measurement campaign. The image acquisition was therefore performed with a fixed frame rate adapted to the propeller rotation speed. The shift between the frame rate and the rotation speed of the propeller led to a slight shift of the blade position in consecutive frames. This still enables to obtain results of the blade deformation at several fixed phase positions but requires intensive manual post-processing for matching the markers with individual recordings, a process which is still ongoing. A reference area was defined between the blade fixed markers on the root to enable a mapping of the measurement results to the undeformed reference surface measured at no wind and no rotation conditions. The deformation (Dz), color-coded in Fig. 14, was determined by subtracting the reference surface from the mapped measurement surface data. Looking to the 4 sample results in Fig. 14 it can be seen that the blade oscillates with amplitudes up to 2.5 mm at the blade tip. Even torsion of the blade can be seen. The bending results show a similar trend with a FEM analysis for static conditions (at higher loading conditions). A strain-

gage was installed on the propeller and integration of the signals of this sensor indicates that the second harmonic nearly coincides with the first flapping mode [16]. This supports the observation of the significant bending oscillation. For an analysis of the bending and torsion behavior of the blade the results must be transferred from the camera fixed coordinate system to a blade fixed coordinate system to enable a well-defined transfer of the acquired data to numerical simulations.

OUTLOOK

The application of simultaneous advanced measurement techniques remains relevant for multiple flow field phenomena. A second measurement campaign with time resolved tomographic PIV and the Acoustic Array technique for acoustic-PIV causality correlation of flap side edge noise has been conducted recently. Figure 15 shows a part of the set-up on the same QESTOL wind tunnel model in the same wind tunnel but in a partially open acoustic wind tunnel configuration (a floor plate was installed for acoustic considerations). A "fat sheet" tomographic measurement with a measurement volume: 390 x 70 x 6 mm^3 and a time resolution up to 3000 vector fields per second were used. Figure 16 and 17 show preliminary results of the tomographic PIV measurement and the acoustic array technique, respectively. The analysis is still ongoing and will focus on correlating the velocity (fluctuation) information with the acoustic pressure signals.

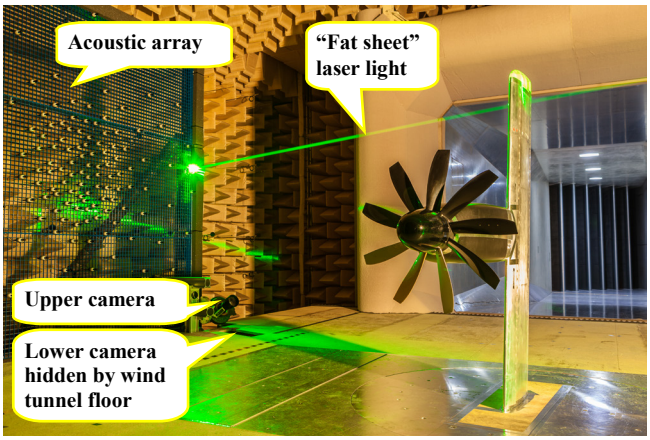

Figure 15 Set-up in open wind tunnel configuration.

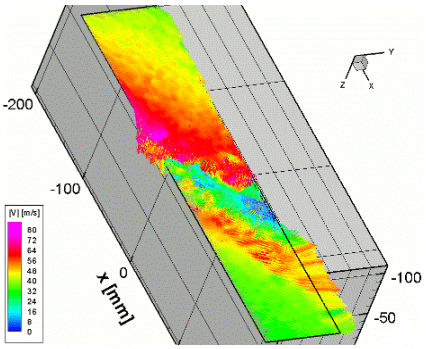

Figure 16 Preliminary time-resolved tomographic PIV result.

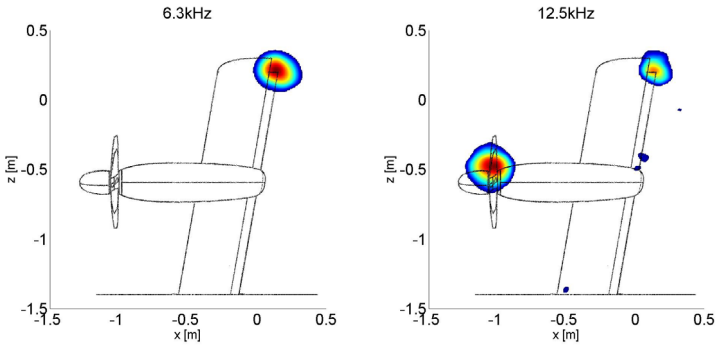

(a) (b)

Figure 17 Preliminary beamforming maps.

CONCLUSIONS

The simultaneous application of multiple advanced image-based measurements techniques has been reported for the investigation of a propeller aircraft with active blowing. The particular design of the aircraft requires experimental input of the various flow features. The main objective is to determine the experimental flow and propeller features simultaneously so that the propeller and wind tunnel properties can be related. In addition the simultaneous acquisition of different flow features establishes a database of experimental data which will be used in a future CFD validation. The applied techniques consisted of: a double stereoscopic Particle Image Velocimetry system (for the investigation of the velocity and vorticity in the propeller slipstream), a mono-PIV system (for investigation of the active blowing flow field), a Background Oriented Schlieren system (for determining the density gradients in the propeller slipstream) and a stereoscopic projected pattern system (for determining the bending and torsion of the propeller blades). Using these techniques a tip vortex roll-up was determined at the location wind leading, in addition to the disjunction of the helical vortex path with the BOS technique. The active blowing was found to induce a higher axial velocity in the propeller

slipstream. The projected pattern results indicate that significant bending of the propeller blade is present. Ongoing work in the project is the correlation of time-resolved tomographic PIV velocity field data (and fluctuations) with acoustic pressure signals (obtained with the Acoustic Array technique) for the investigation of flap edge noise.

APPENDIX A

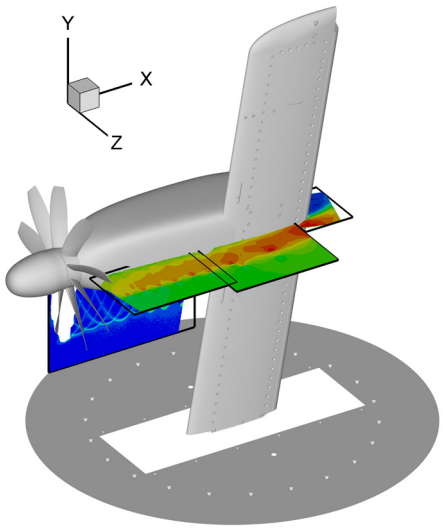

Figure A Combined PIV and BOS results.

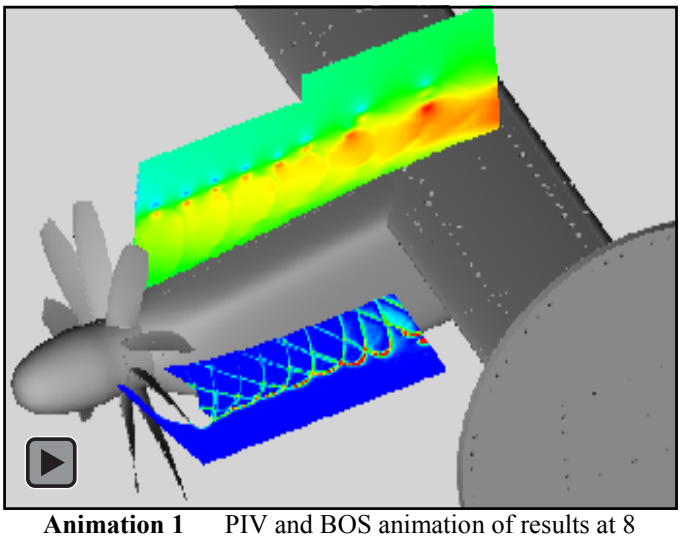

Animation 1 PIV and BOS animation of results at 8 consecutive propeller phase angles (The animation is only available in the digital PDF file).

ACKNOWLEDGMENTS

The work presented here has been carried out within the projects 'Bürgernahes Flugzeug' (established in 2009 and partly funded by the state of Lower Saxony), and 'SAMURAI' (a DLR project). The authors would like to acknowledge Nils Beck (TU Braunschweig, Institute of Fluid Mechanics), Alireza Rezaeian (DLR, Institute of Aeroelasticity) and the wind tunnel team from DNW-NWB for their support during the measurement campaign, Dirk Michaelis (LaVision GmbH) for the tomographic PIV analysis and Arne Henning, Stefan Kröber and Thomas Ahlefeldt (DLR, Institute of Aerodynamics and Flow Technology) for the aero-acoustic measurements and analysis. Please note that the resolution of the images has been drastically reduced in order to keep the file size around 5 MB, as requested by the conference organizers.

REFERENCES

[1] Roosenboom EWM and Schröder A "Image Based Measurement Techniques of Increased Complexity for Industrial Propeller Flow Investigations" 27th AIAA Aerodynamic Measurement and Ground Testing Conference, June 2010, Chicago, IL, USA

[2] Roosenboom EWM and Schröder A "Flowfield Investigation at Propeller Thrust Reverse" Journal of Fluids Engineering (2010) Vol. 132, No. 6 pp. 1-8

[3] Roosenboom EWM, Heider A and Schröder A "Investigation of the Propeller Slipstream with Particle Image Velocimetry" Journal of Aircraft (2009), Vol. 46, No. 2 pp. 442-449

[4] Roosenboom EWM and Schröder A "Qualitative investigation of a propeller slipstream with Background Oriented Schlieren" Journal of Visualization (2009) Vol. 12, No. 2 pp. 165-172

[5] Klein C, Henne U, Sachs W, Hock S, Falk N, Beifuss U, Ondrus V and Schaber S "Pressure Measurement on Rotating Propeller Blades by means of the Pressure-Sensitive Paint Lifetime Method (AIAA 2013-0483)" 51st AIAA Aerospace Sciences Meeting including the New Horizons Forum and Aerospace Exposition, January 2013, Grapevine, TX, USA

[6] Schulein E, Rosemann H and Schaber S "Transition Detection and Skin Friction Measurements on Rotating Propeller Blades (AIAA 2012-3202)" 28th Aerodynamic Measurement Technology,Ground Testing, and Flight Testing Conference , June 2012, New Orleans, LA, USA

[7] Roosenboom EWM, Stürmer A and Schröder A "Advanced Experimental and Numerical Validation and Analysis of Propeller Slipstream Flows" Journal of Aircraft (2010), Vol. 47, No. 1 pp. 284-291

[8] Stürmer A, Marquez Gutierrez CO, Roosenboom EWM, Schröder A, Geisler R, Pallek D, Agocs J, Neitzke K-P "Experimental and numerical investigation of a contra rotating open rotor flow field" Journal of Aircraft (2012), Vol. 49, No. 6, 2012, pp. 1868-1877

[9] Jensch C, Pfingsten KC, Radespiel R, Schuermann M, Haupt M, Bauss S "Design aspects of a gapless high-lift system with active blowing", Deutscher Luft- und Raumfahrtkongress, 2009, Aachen, Germany

[10] Hecker P and Butzmühlen C "Das Bürgernahe Flugzeug" Deutscher Luft- und Raumfahrtkongress, September 2010, Hamburg, Germany

[11] Lenfers C "Propeller Design for a future QESTOL Aircraft in the BNF Project (AIAA 2012-3334)" 30th AIAA Applied Aerodynamics Conference, June 2012, New Orleans, LA, USA

[12] Beck N and R. Radespiel R "Entwurf eines Windkanalexperiments für aktiven Hochauftrieb" Deutscher Luft- und Raumfahrtkongress,

September 2010, Hamburg, Germany
[13] Beck N, Wentrup M and Radespiel R “Realisierung eines Windkanalexperiments für aktiven Hochauftrieb” Deutscher Luft- und Raumfahrtkongress, September 2011, Bremen, Germany
[14] Rezaeian A “Dynamic stability analysis of a propeller-wing wind tunnel model” Deutscher Luft- und Raumfahrtkongress, September 2011, Bremen, Germany
[15] Sutton MA and Orteu JJ and Schreier H “Image Correlation for Shape, Motion and Deformation Measurements: Basic Concepts,Theory and Applications”, ISBN 978-0-387-78746-6, Springer 2009
[16] Rezaeian A “Stability Assessment of a Propeller-Wing Wind Tunnel Model Based on Analysis Using Measured Structural Data and Online-Monitoring” International Forum on Aeroelasticity and Structural Dynamics (IFASD), June 2013, Bristol, England (submitted for publication)